Formation of Nanoparticle-Loaded Microcapsules Based on Hydrogen-Bonded Multilayers

Daeyeon Lee,[†] Michael F. Rubner,*[,‡] and Robert E. Cohen*[,†]

Department of Chemical Engineering and Department of Materials Science and Engineering and the Center for Materials Science and Engineering, Massachusetts Institute of Technology, 77 Massachusetts Avenue, Cambridge, Massachusetts 02139

Received September 9, 2004. Revised Manuscript Received December 15, 2004

We show that hydrogen-bonded multilayer thin film coatings assembled on colloidal particles can be used as templates for the in situ synthesis of nanoparticles. The concentration and size of nanoparticles grown within the coatings can be tuned by the number of loading cycles. The hydrogen-bonded multilayer thin films were coated on polystyrene micrometer-sized colloidal particles and subsequently cross-linked via water-soluble carbodiimide chemistry. We show that metal nanoparticles (e.g., Ag and Pd) can be synthesized via the nanoreactor scheme, where corresponding metal ions are loaded into the coating and then subsequently reduced to create nanoparticles dispersed within the coating. In addition, we demonstrate the multiple loading capability of the hydrogen-bonded multilayer coatings. UV−vis spectroscopy and direct observation by transmission electron microscopy confirm that the nanoparticles are well-dispersed within the thin film coating. Finally, the polystyrene particles can be extracted by treating the nanocomposite-coated particles with tetrahydrofuran or toluene, leaving the nanoparticles embedded within the resultant multilayer hollow microcapsule walls.

Introduction

The formation of nanoparticle-loaded thin films has been an active area of research for a number of years.[1] Nanometer-sized metal particles have unusual properties that originate from quantum confinement effects and their large specific surface area.[2] Possible applications for nanoparticles dispersed in an organic matrix include catalysis,[3,4] magnetics,[5,6] and photonics.[7,8] The formation of nanoparticle-loaded polymer coatings on colloidal particles is a desirable goal since colloidal particles provide extra surface area that can be advantageous for various applications such as catalysis[3] and sensor applications.[9] In addition, the added function provided by the nanoparticles further expands the utility of colloidal particles.

A frequently utilized method to create nanoparticle-loaded thin film coatings on colloidal particles is via layer-by-layer (LbL) assembly of a polyelectrolyte and preformed nanoparticles of an opposite surface charge.[10,11] While this approach provides a simple route to creating nanocomposite coatings, nanoparticles must be functionalized for dispersion in water and control of the particle concentration in the coatings is difficult to achieve. In another approach, Sukhorukov and co-workers have demonstrated that nanocomposite hollow microcapsules can be formed by precipitating inorganic materials exclusively inside the hollow microcapsules composed of poly(styrene sulfonate) (SPS) and poly(allylamine hydrochloride) (PAH).[12,13]

We have developed a general technique for in situ nanoparticle synthesis in polyelectrolyte multilayer (PEM) films and heterostructures, capitalizing on the pH-dependent properties of PEM films assembled from weak polyelectrolytes;[14,15] the methodology is an extension of our earlier work in which carboxylic acid functionalized block copolymers provided nanoreactor templates for inorganic cluster synthesis.[16−18] The LbL assembly conditions were tuned so that the multilayer thin films have a significant content of nonionized carboxylic acid groups that have not been

* To whom correspondence should be addressed. E-mails: rubner@mit.edu (M.F.R.); recohen@mit.edu (R.E.C.).

[†] Department of Chemical Engineering.

[‡] Department of Materials Science and Engineering and the Center for Materials Science and Engineering.

(1) Fendler, J. H. *Nanoparticles and Nanostructured Films: Preparation, Characterization and Applications*; Wiley-VCH Verlag GmbH: Weinheim, Germany, 1998.
(2) Alivisatos, A. P. *Science* **1996**, *271*, 933−937.
(3) Kidambi, S.; Dai, J. H.; Li, J.; Bruening, M. L. *J. Am. Chem. Soc.* **2004**, *126*, 2658−2659.
(4) Ciebien, J. F.; Cohen, R. E.; Duran, A. *Supramol. Sci.* **1998**, *5*, 31−39.
(5) Ziolo, R. F.; Giannelis, E. P.; Weinstein, B. A.; Ohoro, M. P.; Ganguly, B. N.; Mehrotra, V.; Russell, M. W.; Huffman, D. R. *Science* **1992**, *257*, 219−223.
(6) Sohn, B. H.; Cohen, R. E.; Papaefthymiou, G. C. *J. Magn. Magn. Mater.* **1998**, *182*, 216−224.
(7) Beecroft, L. L.; Ober, C. K. *Chem. Mater.* **1997**, *9*, 1302−1317.
(8) Wang, T. C.; Cohen, R. E.; Rubner, M. F. *Adv. Mater.* **2002**, *14*, 1534−1537.
(9) Duchesne, T. A.; Brown, J. Q.; Guice, K. B.; Lvov, Y. M.; McShane, M. J. *Sens. Mater.* **2002**, *14*, 293−308.
(10) Caruso, F.; Caruso, R. A.; Möhwald, H. *Science* **1998**, *282*, 1111−1114.
(11) Donath, E.; Sukhorukov, G. B.; Caruso, F.; Davis, S. A.; Möhwald, H. *Angew. Chem., Int. Ed.* **1998**, *37*, 2202−2205.
(12) Shchukin, D. G.; Sukhorukov, G. B.; Möhwald, H. *Angew. Chem., Int. Ed.* **2003**, *42*, 4472−4475.
(13) Shchukin, D. G.; Sukhorukov, G. B. *Adv. Mater.* **2004**, *16*, 671−682.
(14) Joly, S.; Kane, R.; Radzilowski, L.; Wang, T.; Wu, A.; Cohen, R. E.; Thomas, E. L.; Rubner, M. F. *Langmuir* **2000**, *16*, 1354−1359.
(15) Wang, T. C.; Rubner, M. F.; Cohen, R. E. *Langmuir* **2002**, *18*, 3370−3375.
(16) Kane, R. S.; Cohen, R. E.; Silbey, R. *Chem. Mater.* **1996**, *8*, 1919−1924.
(17) Kane, R. S.; Cohen, R. E.; Silbey, R. *Chem. Mater.* **1999**, *11*, 90−93.
(18) Yue, J.; Cohen, R. E. *Supramol. Sci.* **1994**, *1*, 117−122.

10.1021/cm048441v CCC: $30.25
Published on Web 02/04/2005

compensated for by positive functional groups (e.g., charged amine groups). Protons of these carboxylic acid groups are then replaced by metal ions by a simple aqueous exchange procedure. Subsequently, the metal ions are converted into metal or semiconductor nanoparticles, creating nanoparticle-loaded thin films. Nanoreactor chemistry is a versatile method in which a single template can be used to synthesize various inorganic nanoparticles and, at the same time, control the size, concentration, and spatial location.

The extension of nanoreactor chemistry to create uniform nanoparticle-loaded thin film coatings on colloidal particles, however, has been troublesome due to the difficulty faced in forming LbL-assembled coatings with a high amount of uncompensated carboxylic acid groups. As Caruso and co-workers have reported, colloids with multilayer thin film coatings assembled from weak polyelectrolytes tend to undergo irreversible coagulation when either of the polyelectrolytes has a low degree of ionization.[19] This same group[20] has overcome the undesirable aggregation problem and achieved weak polyelectrolyte multilayer coatings on colloidal particles by utilizing copper-assisted[21] electrostatic LbL assembly, and they have recently successfully synthesized a variety of nanoparticles in the coatings.[22]

Hydrogen-bonded multilayer systems containing pH-sensitive weak polyelectrolytes provide an alternative opportunity for creating nanoparticle-loaded thin films on various substrates.[23,24] We and others have shown that hydrogen-bonded systems can be used to build multilayer thin film coatings on colloidal particles while avoiding irreversible aggregation of the coated particles.[25,26] As will be demonstrated in this work, the high content of free carboxylic acid groups in these systems can be utilized for further chemistry. Multilayer thin films fabricated from weak polyelectrolytes using hydrogen-bonding interactions must be built at conditions in which most of the carboxylic acid groups of weak polyacids (e.g., poly(acrylic acid)) are in the nonionized state during the LbL assembly. The high content of carboxylic acid groups within the multilayers makes these systems ideally suited for nanoreactor chemistry. To use the hydrogen-bonded weak polyelectrolyte multilayers as templates for nanoreactor chemistry, however, the multilayers must be cross-linked to prevent dissolution under pH conditions that ionize the functional groups of the weak polyelectrolyte. We have accomplished this stabilization using water-soluble carbodiimide chemistry.[26]

In previous work, we demonstrated that solution cross-linked, hydrogen-bonded multilayer coatings composed of a weak polyelectrolyte (poly(acrylic acid)) and a neutral polymer (polyacrylamide) can be produced successfully on colloidal particles; the multilayer-modified colloids showed interesting cell-adhesion resistance.[26] In this report, we show that solution-cross-linked hydrogen-bonded multilayer coatings composed of poly(acrylic acid) and polyacrylamide can be used successfully as templates for nanoreactor chemistry on polymer colloidal particles. UV−vis spectroscopy confirms that multilayer thin films can be used as templates for nanoreactor chemistry. Transmission electron microscopy (TEM) images of the thin sections of core particles with the nanoparticle-loaded multilayer coatings show that the metal nanoparticles are highly dispersed in the polymer coatings. We also show that it is possible to create nanoparticle-loaded hollow microcapsules by dissolving away the core particles.

Experimental Section

Materials. Poly(acrylic acid) (PAA; $M_w \sim 90\,000$, 25% aqueous solution) and polyacrylamide (PAAm; $M_w \sim 800\,000$, 10% aqueous solution) were purchased from Polysciences. Two samples of amine-functionalized polystyrene (amine-PS) spherical particles (2.5 wt % aqueous solution) were purchased from Polysciences; the particle diameters were specified as 3.18 and 5.8 μm by the supplier. 1-Ethyl-3-(3-(dimethylamino)propyl)carbodiimide hydrochloride (EDC) was purchased from Pierce Biotechnology. Silver acetate, tetraaminepalladium(II) chloride monohydrate ($[Pd(NH_3)_4]Cl_2 \cdot H_2O$), dimethylamine borane (DMAB), and sodium borohydride ($NaBH_4$) were purchased from Sigma-Aldrich. All chemicals were used as received.

Multilayer Coating of Colloidal Particles. Details about the deposition and cross-linking of PAA/PAAm multilayer thin film coatings on colloidal particles have been published previously.[26] In brief, all solutions (20 mM based on the repeat unit) were adjusted to a low pH with 0.1 M HCl. Amine-PS particles were suspended in a low-pH PAA solution (either pH 3.0 or 3.2) with agitation for 10 min and then settled by using a centrifuge. After the polymer solution was removed by decantation, the colloids were rinsed with water of the same pH two times with brief sonication (<1 min). The colloidal particles were then resuspended in the next polymer solution, and the process was repeated to deposit multilayer coatings.[27] Cross-linking of PAA/PAAm multilayer coatings was accomplished by the previously reported method.[26] For cross-linking of the coatings, a 100 mg/mL EDC stock solution (at the same pH as the assembly condition) was made and 30 μL of the stock solution was added into a 1 mL dilute suspension of coated colloidal particles. The suspension was agitated overnight (~10 h) and washed with deionized (DI) water (pH 5−6) several times. For core template dissolution, the coated particles were resuspended in tetrahydrofuran (THF) or toluene for 30 min and then washed with respective solvent twice and with DI water two times.

In Situ Synthesis of Nanoparticles via Nanoreactor Chemistry. After the thin film coatings were cross-linked by EDC treatment, metal ions were bound to the carboxylic acid groups within the thin film coatings by suspending the coated amine-PS particles in metal ion containing aqueous solutions. Specifically, particles were suspended in 5 mM aqueous solutions of silver acetate or tetraaminepalladium(II) chloride for 30 min. After metal ion loading, the particles were washed thoroughly with DI water three times with brief sonication. Rinsed particles were then resuspended in 1 mM DMAB(aq) or 1 mM $NaBH_4$(aq) for 5 min. The solution pH of 1 mM DMAB(aq) and 1 mM $NaBH_4$(aq) was measured to be pH 7.5 and 9.5, respectively. The color of coated

(19) Kato, N.; Schuetz, P.; Fery, A.; Caruso, F. *Macromolecules* **2002**, *35*, 9780−9787.
(20) Schuetz, P.; Caruso, F. *Adv. Funct. Mater.* **2003**, *13*, 929−937.
(21) Balachandra, A. M.; Dai, J. H.; Bruening, M. L. *Macromolecules* **2002**, *35*, 3171−3178.
(22) Schuetz, P.; Caruso, F. *Chem. Mater.* **2004**, *16*, 3066−3073.
(23) Sukhishvili, S. A.; Granick, S. *Macromolecules* **2002**, *35*, 301−310.
(24) Yang, S. Y.; Rubner, M. F. *J. Am. Chem. Soc.* **2002**, *124*, 2100−2101.
(25) Kozlovskaya, V.; Ok, S.; Sousa, A.; Libera, M.; Sukhishvili, S. A. *Macromolecules* **2003**, *36*, 8590−8592.
(26) Yang, S. Y.; Lee, D.; Cohen, R. E.; Rubner, M. F. *Langmuir* **2004**, *20*, 5978−5981.

(27) All future references to the multilayer thin films in this report will be denoted as "$(PAA/PAAm)_x$", where the x is the number of bilayers.

Scheme 1. Formation of Nanoparticle-Loaded Hollow Microcapsules Based on Hydrogen-Bonded Multilayers[a]

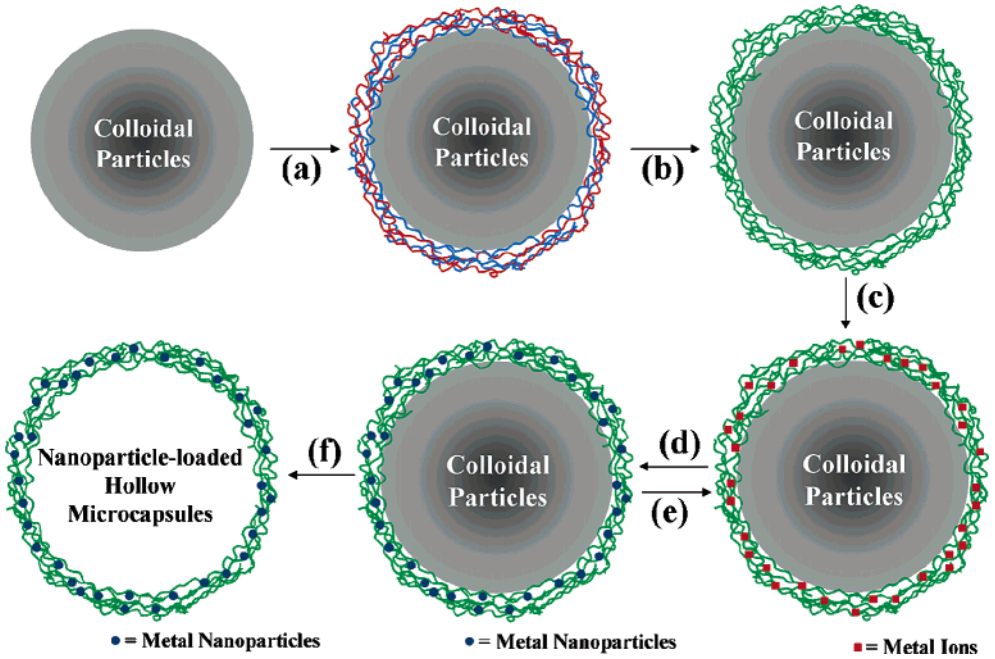

[a] (a) Layer-by-layer assembly of (PAA/PAAm) multilayer thin film coatings, (b) cross-linking using water-soluble carbodiimide (i.e., EDC), (c) binding selective metal ions from aqueous solutions, (d) reduction of metal ions to zerovalent nanoparticles in DMAB(aq) or $NaBH_4$(aq) and regeneration of carboxylic acid groups for further loadings,[18,28] (e) reloading selective metal ions from aqueous metal ion solutions, and (f) dissolution of the amine-PS particles using an organic solvent (e.g., THF or toluene).

particles loaded with silver and palladium turned to reddish brown and dark black after 5 min, respectively. The coated particles after reduction were rinsed with DI water three times. For multiple loadings,[18,28] rinsed particles were subjected to the original sequence of treatments. Nanoparticle-loaded hollow microcapsules could be obtained by treating the particles with nanoparticle-loaded coatings with THF or toluene for at least 30 min. Scheme 1 shows the steps involved in creating nanoparticle-loaded thin film coatings on colloidal particles and subsequently the microcapsules.

Transmission Electron Microscopy. TEM images were generated on a JEOL 200 CX operated at 200 kV. The suspension of colloidal particles with metal nanoparticle-loaded thin film coatings was dehydrated and subsequently embedded in epoxy for microtoming. Ultrathin sections (70−100 nm) for TEM observation were microtomed at room temperature with a glass or diamond knife using a RMC MT-X ultramicrotome and collected on copper grids. To image microcapsules in plan view, THF-treated particles were resuspended in DI water and then deposited on carbon-coated copper grids and allowed to dry in ambient conditions.

UV−Visible Spectroscopy. A Varian Cary 6000i UV−vis−near-IR spectrometer was used to measure the UV−vis spectra of multilayer thin films deposited on quartz slides (both sides). Details of the multilayer thin film assembly on planar substrates can be found elsewhere.[26,29] To enhance the absorbance intensity, $(PAA/PAAm)_{10}$ multilayer thin films were assembled at pH 3.0 with a PAH layer as a primer layer to ensure the film assembly. After the films were assembled, the nanoparticles were created in the thin films following the same procedure as that for the polyelectrolyte multilayer coated colloidal particles.

Results and Discussion

The feasibility of using the solution-cross-linked hydrogen-bonded (PAA/PAAm) multilayer thin films as templates for nanoreactor chemistry was examined and confirmed by UV−vis spectroscopy of the cross-linked multilayer thin films on quartz slides. As shown in Figure 1, when the EDC-cross-linked $(PAA/PAAm)_{10}$ multilayer thin films are loaded with metal ions, the UV−vis spectra for Ag^+-loaded thin films

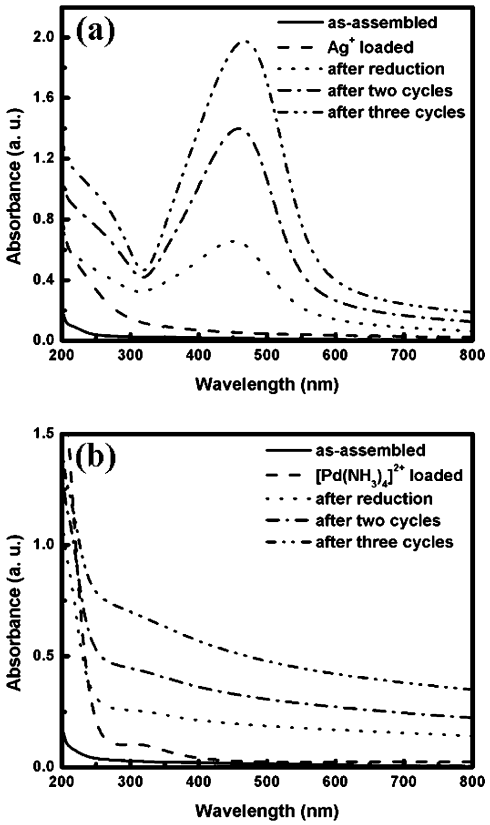

Figure 1. UV−vis spectra of $(PAA/PAAm)_{10}$ multilayer thin films assembled on quartz slides: (a) Ag- and (b) Pd-loaded and reduced films.

(28) Clay, R. T.; Cohen, R. E. *Supramol. Sci.* **1997**, *4*, 113−119.
(29) Yang, S. Y.; Mendelsohn, J. D.; Rubner, M. F. *Biomacromolecules* **2003**, *4*, 987−994.

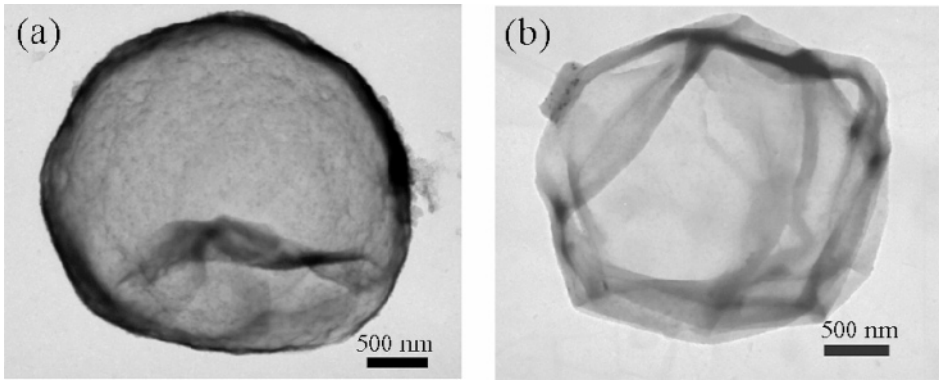

Figure 2. TEM images of PAA/PAAm microcapsules (five bilayers) assembled at pH 3.0, (a) without cross-linking and (b) with cross-linking. The diameter of the extracted amine-PS particles was 3.18 μm. (Each figure represents a majority of microcapsule morphologies observed under TEM.)

do not show any significant peaks, whereas the $[Pd(NH_3)_4]^{2+}$-loaded films show a broad peak around 320 nm corresponding to palladium ions in the polymer thin film. Upon reduction, the UV−vis spectra of the silver-loaded films show the appearance of a surface plasmon resonance (SPR) peak at 450 nm.[30] A slight red shift in the SPR peak compared to the value reported (∼435 nm) in a previous paper[15] suggests that the solution-reduced Ag nanoparticles grow to larger sizes in the hydrogen-bonded multilayers compared to the hydrogen-reduced Ag nanoparticles in multilayers composed of PAA and PAH or that small nanoparticles agglomerate into larger clusters in the hydrogen-bonded templates.[31] Formation of somewhat larger Ag nanoparticles is also corroborated by TEM observation as described below. As for palladium nanoparticles, it is known that the UV−vis spectrum is influenced only by Mie scattering without any SPR peak. The Mie scattering leads to an increase in the absorbance throughout the entire UV−vis region.[32,33]

To confirm the multiple loading capability of the hydrogen-bonded multilayer thin films, Ag and Pd nanoparticles were loaded and reduced up to three times. As can be seen in Figure 1a, the intensity of the SPR band of the nanoparticle-loaded films increased with the number of loading and reduction cycles of Ag similar to a previous report by Wang et al.[15] The SPR band of the Ag nanoparticles also shifts to higher wavelength, reflecting the fact that the size as well as the interparticle interaction of the nanoparticles increased as the number of loading and reduction cycles was increased.[31] Figure 1b shows that, in the case of Pd nanoparticles, the absorbance intensity of a broad band across the entire UV−vis region increases, reflecting the increase in the amount of Pd nanoparticles within the film. The UV−vis spectra of Ag and Pd nanoparticle-loaded films do not show significant change after 1 month in ambient air, which suggests that in situ synthesized Ag and Pd nanoparticles were stable against oxidation within the films.

Depending on the size of the amine-PS particles, irreversible aggregation of the multilayer-coated particles during LbL assembly could be eliminated by tuning the solution pH of each polymer solution. For 5.8 μm amine-PS particles, the films were assembled with up to 12 layers (six bilayers) without any aggregation problems at pH 3.0. When the 3.18 μm amine-PS particles were coated at pH 3.0, however, we observed that the particles showed some degree of aggregation after the eighth layer. To avoid the aggregation of the 3.18 μm amine-PS particles during the LbL process, the pH of each polymer solution as well as the rinse solution was raised to pH 3.2. At this pH, we did not observe any aggregation problems up to six bilayers. A slight increase in the assembly pH imparts an additional small amount of negative charge on the surface of coated colloids, which is sufficient to maintain the colloidal stability against irreversible aggregation.[26] However, we expect a decrease of ca. 25% in the film thickness based on quartz crystal microbalance (QCM) experiments (not shown) conducted at the two different pH conditions. If the size of the colloidal particles is further reduced below 1 μm, the colloidal suspension becomes more susceptible to irreversible aggregation during the LbL assembly. As shown in Figure 2a, as-assembled $(PAA/PAAm)_6$ multilayer coatings on particles were intact even after the amine-PS particles were dissolved away by THF treatments and we were able to obtain microcapsules that retain the approximate size of the original amine-PS particles.

As was reported previously, the cross-linking of PAA/PAAm multilayer thin films with a low concentration of EDC at low pH renders the multilayer thin films stable even at high-pH conditions above pH 7.[26] Figure 2b demonstrates that microcapsules were stable against dissolution after cross-linking the coatings with EDC and treating them with pH 7 adjusted DI water. Non-cross-linked hydrogen-bonded multilayer coatings dissolved away in pH 7 adjusted DI water, and we could not observe any capsules after the amine-PS particles were dissolved away in THF or toluene. The surface topologies of microcapsules before and after cross-linking are strikingly different. As can be clearly seen in Figure 2, the as-assembled capsules have a few folds and creases after they were dried on TEM grids, whereas the EDC-cross-linked microcapsules have many folds and creases after drying. We believe that the cross-linking of the PAA/PAAm multilayer coatings prevents the chains from rearranging while the capsules are being dried and, in turn, decreases the ability of the capsule wall to respond to abrupt changes in the

(30) Ohde, H.; Hunt, F.; Wai, C. M. *Chem. Mater.* **2001**, *13*, 4130−4135.
(31) Kreibig, U.; Vollmer, M. *Optical Properties of Metal Clusters*; Springer-Verlag: New York, 1995; Vol. 25.
(32) Chen, S. W.; Huang, K.; Stearns, J. A. *Chem. Mater.* **2000**, *12*, 540−547.
(33) Ohde, H.; Wai, C. M.; Kim, H.; Kim, J.; Ohde, M. *J. Am. Chem. Soc.* **2002**, *124*, 4540−4541.

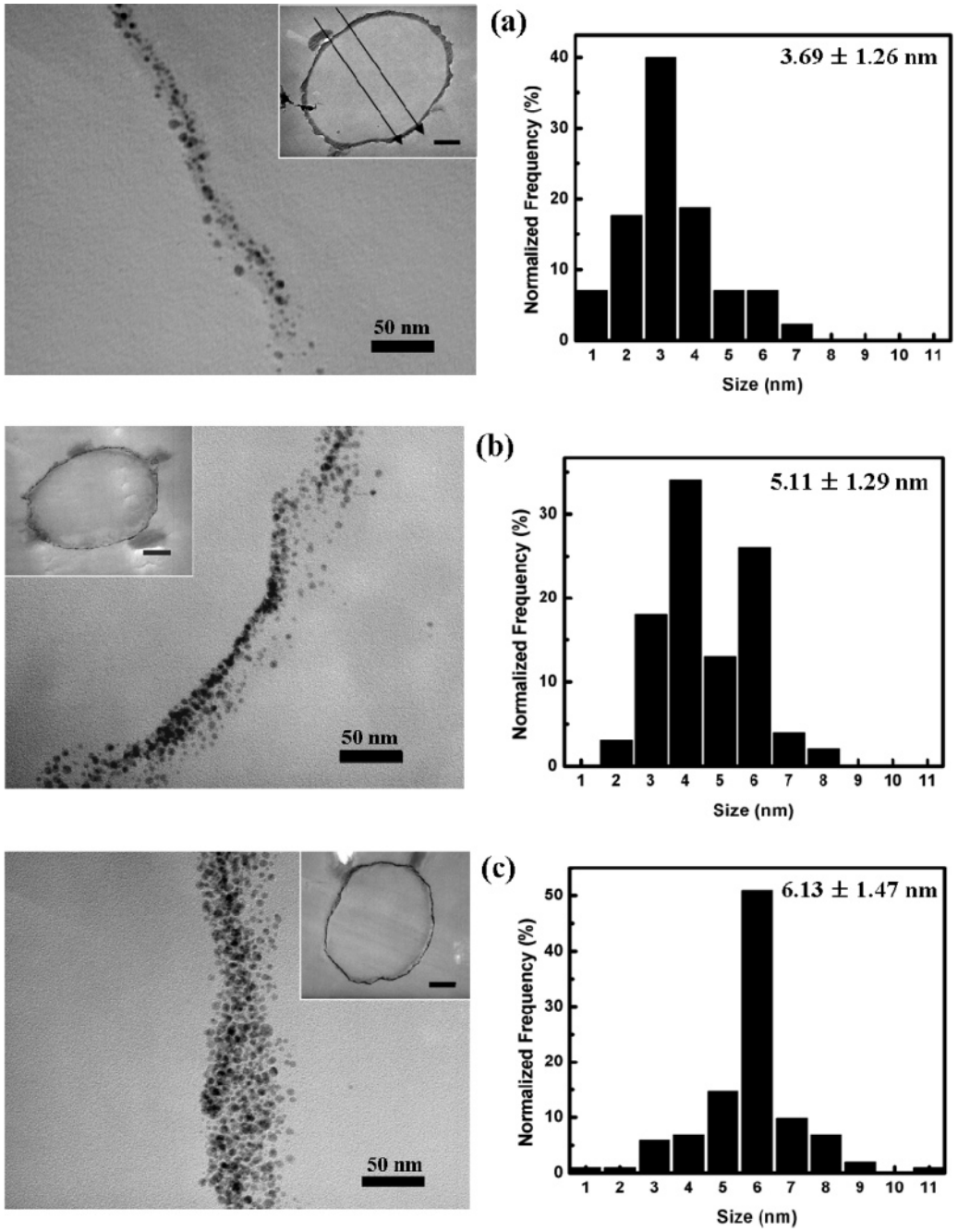

Figure 3. Cross-section TEM images of $(PAA/PAAm)_6$ Ag nanoparticle-loaded coatings assembled at pH 3.0 on 3.18 μm amine-PS particles (a) after the first loading and reduction cycle (arrows show the direction of knife marks), (b) after the second cycle, and (c) after the third cycle. Inset scale bars are 500 nm. Histograms show the size distribution of Ag nanoparticles measured from each TEM image. Average particle size is denoted in each histogram along with standard deviation (approximately 100 nanoparticles were measured to produce the histograms; while showing the size distribution of Ag nanoparticles, these histograms are not necessarily the true statistical representation of the entire Ag nanoparticle size distribution).

environment such as would occur during dehydration. Additionally, Pavoor et al. have recently reported that the wet-state modulus and hardness of thermally cross-linked polyelectrolyte multilayer thin films composed of PAA and PAH are significantly higher than those observed for wet, un-cross-linked PAA/PAH multilayer thin films.[34] The cross-linking of hydrogen-bonded PAA/PAAm multilayers is expected to have a similar effect on the mechanical properties of these capsule walls, leading to significantly different capsule morphologies as they are dried from aqueous suspension. On the other hand, as-assembled hydrogen-bonded multilayer hollow capsules without cross-linking may find use in applications where the coatings are intact at low-pH conditions and then dissolve away, exposing the core at high-pH conditions.

The presence of Ag nanoparticles within the EDC cross-linked PAA/PAAm multilayer thin film coatings was confirmed by TEM. Figure 3 shows the cross-section TEM images of the nanoparticle-loaded thin film coatings on 3.18 μm amine-PS particles. The nanoparticle-loaded coating conformably coats the entire surface of the amine-PS particles. Also the magnified images clearly show that the

(34) Pavoor, P. V.; Bellare, A.; Strom, A.; Yang, D.; Cohen, R. E. *Macromolecules* **2004**, *37*, 4865−4871.

particles are highly dispersed within the multilayer coating. As the number of loading cycles was increased, the density as well as the size of the Ag nanoparticles increased. The size of the particles is greater than that observed in a previous study where the loaded metal ions in electrostatically assembled weak polyelectrolyte multilayer thin films of PAA and PAH on planar substrates were reduced in $H_2(g)$.[15] We suspect that the aqueous phase reaction imparts more mobility to the metal ions during reduction. In addition, the cross-linked PAA/PAAm multilayers are known to swell in a high-pH aqueous environment. The solution pH of both of the reducing agents was above 7.0. The swelling of the coatings can provide more mobility within the polymer matrix, thereby allowing larger particles to form compared to the denser polymer matrix present in the gas-phase reduction.

Cross-section TEM images in Figure 3 provide additional information about the nanoparticle-loaded coatings on the microparticles. First of all, the thickness of the thin film coatings on the particles can be estimated by measuring the thickness of the nanoparticle-loaded coatings. The thickness measured from the TEM images for a six-bilayer coating of PAA/PAAm assembled at pH 3.0 after one loading and reduction cycle is ~28 nm (Figure 3a), which is a bit larger than the thickness of the same multilayer thin film assembled on a planar substrate without any metal nanoparticle incorporation (~26 nm). The thickness of multilayer thin films increases as the number of loading and reduction cycles in a multilayer coating is increased, which was also observed by Wang et al.[15] In addition, it has been previously reported that ultramicrotomy can increase a film thickness by 10% compared to that measured using an ellipsometer.[8] The slight increase in the thickness of multilayers on spherical particles compared to that of multilayers on planar substrates is in contrast to a previous report by Kozlovskaya et al.[25] They reported that the thickness, determined by electron energy loss spectrometry (EELS), of hydrogen-bonded multilayers (composed of poly(ethylene oxide)/poly(methacrylic acid) and poly(ethylene oxide)/poly(*N*-vinylpyrrolidone)) assembled on cadmium carbonate ($CdCO_3$) spherical particles was substantially less than that of the same multilayers assembled on planar Si substrates. It should also be noted that the nanocomposite-coated particles appear to have experienced some longitudinal deformation during the sectioning process. The long axis of the resultant deformed ellipsoid is perpendicular to knife marks visible on the thin sections, which corroborates the fact that ultramicrotomy caused deformation of the embedded particles. Similar deformation due to ultramicrotoming has been observed for PAH/SPS multilayer coated colloidal particles.[11] We also believe that the ultramicrotomy of metal-ion stained multilayer coatings on spherical particles will provide a means to measure the thickness of these coatings.

Hollow microcapsules with nanoparticles dispersed within the capsule walls could be obtained by treating the nanocomposite-coated particles with THF or toluene for at least 30 min. Parts a and b of Figure 4 show that nanoparticles of Ag and Pd are well-dispersed within the capsule wall; however, we did observe some loss in the amount of Ag nanoparticles within the cross-linked (PAA/PAAm) multilayer thin films if THF treatment was prolonged beyond 24 h. UV−vis spectra of the Ag nanoparticle-loaded thin films on glass slides that were immersed in THF for 24 h showed a decrease (more than 10%) in the intensity of the silver SPR peak around 450 nm (not shown). After a week in THF, the Ag nanoparticle density (based on UV−vis measurement) was roughly half of its original value. When Pd nanoparticle-loaded coatings are exposed to THF for more than 1 h, the density of Pd nanoparticles in the capsules was substantially less (ca. 30%) than that found in 30 min treated capsules on the basis of TEM observation. A similar trend was seen when toluene, which is less polar than THF, was used for core template extraction. The fact that use of these two different organic solvents gives similar results indicates that the nanoparticles are diffusing out of the multilayer rather than being dissolved by organic solvents during the organic solvent treatment. Therefore, to retain the nanoparticles within the nanocomposite coatings, it is essential to minimize the time required to extract the amine-PS particles out of the multilayer coating.

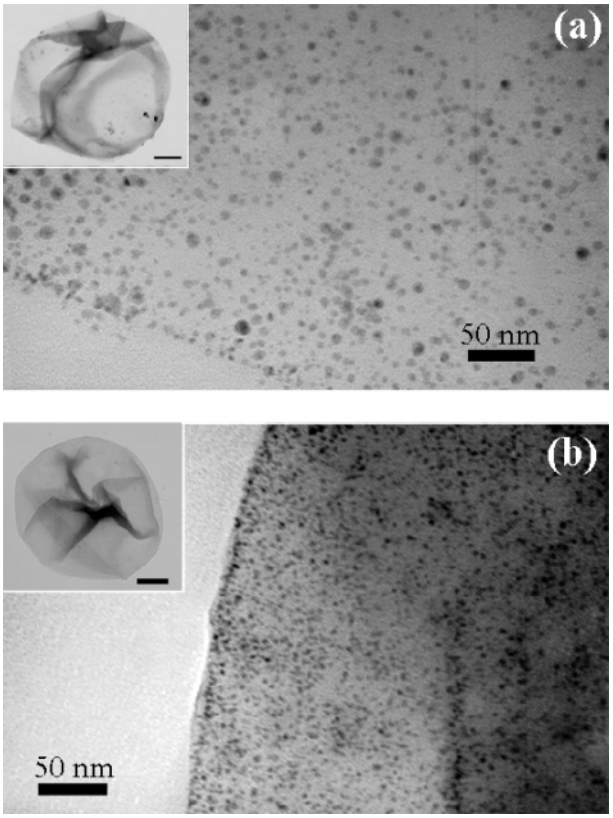

Figure 4. TEM images of EDC-cross-linked $(PAA/PAAm)_5$ multilayer hollow capsules assembled at pH 3.0 and loaded with (a) two loading and reduction cycles of Ag nanoparticles (the diameter of extracted amine-PS particles was 5.8 μm; inset scale bar = 1.2 μm) and (b) one loading and reduction cycle of Pd nanoparticles (the diameter of extracted amine-PS particles was 3.18 μm; inset scale bar = 700 nm).

The size and the density of nanoparticles within the capsule walls differ for different systems. Figure 4a shows that when loading and reduction cycles were repeated twice for Ag-loaded hollow capsules, the size of particles is approximately 5−6 nm, which is close to the size of nanoparticles seen in the cross-section images in Figure 3b. The size of Pd nanoparticles is approximately 1−2 nm, which is smaller

than that of the Ag nanoparticles after one loading and reduction cycle (Figure 3a). The amount of divalent cations that can be exchanged with the protons of the carboxylic acid groups is half the amount of monovalent ions. Also the mobility of divalent metal ions in a carboxylic acid rich polymer thin film matrix is expected to be considerably lower than that of monovalent ions, which, in turn, prevents the growth of larger particles. Clay and Cohen have reported that the diffusion of divalent metal cations is much slower than that of monovalent cations within carboxylic acid group rich domains of microphase-separated block copolymers.[28] Kane et al. also have presented models that predict the size of in situ synthesized nanoparticles to be dependent of the diffusion of metal ions within polymer matrix.[35]

Conclusions

In conclusion, we demonstrated a general methodology for creating nanoparticle-loaded thin film coatings on micrometer-sized colloidal particles based on the layer-by-layer assembly of hydrogen-bonded multilayer thin films and subsequent nanoreactor chemistry. This technique enabled control over the size as well as the amount of loaded metal nanoparticles within the thin film coating. Cross-linked hydrogen-bonded multilayer thin film coatings are robust enough to withstand the high-pH environment during the reduction step. Subsequent core particle extraction can be used to obtain hollow capsules with a high dispersion of nanoparticles within the capsule walls.

The major advantage of our approach in creating nanoparticle-loaded microcapsules lies in the generality of the method. As reported previously, the nanoreactor chemistry can also be extended to synthesize semiconductor nanoparticles such as CdS, ZnS, and PbS in a polymer matrix. In addition, producing nanoparticle-loaded coatings with more than one inorganic component in the polymer matrix should be readily achievable by loading different metal ions in each loading step. Currently, the antimicrobial properties of Ag nanoparticle-loaded coatings and useful applications of other metal-loaded capsules are being investigated.

Acknowledgment. This work was supported by the MIT MRSEC program of the National Science Foundation (Grant DMR 03-13282) and the DuPont-MIT Alliance. The authors thank the Center for Materials Science and Engineering (CMSE) and the Institute for Soldier Nanotechnology (ISN) for use of their characterization tools. We also thank Adam Nolte, Paul Albertus, and Dr. Sung Yun Yang for preliminary studies and helpful discussions on the solution-based reduction chemistry.

CM048441V

(35) Kane, R. S.; Cohen, R. E.; Silbey, R. *Langmuir* **1999**, *15*, 39−43.